JOURNAL OF APPLIED ELECTROCHEMISTRY 26 (1996) 353–359

Meniscus shape and lateral wetting at the hanging meniscus rotating disc (HMRD) electrode

H. M. VILLULLAS*, M. LOPEZ TEIJELO

INFIQC, Depto. de Físico Química, Facultad de Ciencias Químicas, Universidad Nacional de Córdoba, Suc.16, C.C.61, 5016 Córdoba, Argentina

Received 28 June 1995; revised 30 August 1995

The hanging meniscus rotating disc (HMRD) electrode is a configuration in which a cylinder of the electrode material is used without an insulating mantle. We have recently shown that the hydrodynamic behaviour of the HMRD is similar to that of the conventional rotating disc electrode and that this configuration can also be used to study the kinetics of simple charge transfer reactions. In this paper experimental data on the change of meniscus shape upon meniscus height and rotation for different electrode materials are presented and analysed in relation to lateral wetting and stability.

List of symbols

A	electrode area (cm^2)
C_0^*	bulk concentration ($mol\,cm^{-3}$)
D_0	diffusion coefficient ($cm^2\,s^{-1}$)
f	force on a cylinder supporting a hanging meniscus (dyn)
F	Faraday (96 500 $C\,mol^{-1}$)
g	gravitational acceleration ($cm\,s^{-2}$)
h	height (cm)
h_m	meniscus height (cm)
h_0	critical meniscus height (cm)
i	total current (A)
i_L	limiting current (A)
i_{max}	kinetic current (A)
k	proportionality constant (cm^{-1})
K	dimensionless constant
n	number of electrons exchanged
R_{eff}	effective radius of the electrode (cm)
R_0	geometric radius of the electrode (cm)
V	volume of the meniscus above the general level of the liquid surface (cm^3)

Greek letters

δ_0	thickness of hydrodynamic boundary layer (cm)
γ	surface tension ($dyn\,cm^{-1}$)
ν	kinematic viscosity ($cm^2\,s^{-1}$)
ρ	density difference between the liquid and its surrounding fluid ($g\,cm^{-3}$)
θ_C	'normal' contact angle
θ_L	local contact angle
ϕ	$\theta_L + 90°$
ω	electrode rotation rate (s^{-1})

1. Introduction

The rotating disc electrode (RDE) [1] has been widely used in research in electrochemistry [2–4]. The RDE is traditionally constructed by press-fitting the electrode material into an insulating mantle, usually Teflon or another plastic. However, this procedure is not always possible and/or convenient for electrode materials for which mechanical stresses produced when the electrode is encased must be avoided. An extreme example of this problem is found for metal single crystals where severe damage of crystal structure could be produced.

After the introduction of the pendant meniscus in electrochemistry by Dickertmann *et al.* [5], the use of a static hanging meniscus of electrolyte to prevent undesired contributions from the electrode side, has been extensive in research on single crystal electrodes [6]. To make possible the mounting of single crystals as rotating electrodes without having to face the problems associated with press-fitting and other procedures for encasing the electrode material, the hanging meniscus rotating disc (HMRD) has recently been developed [7, 8]. The HMRD uses a cylinder with no external shroud which is simply lowered until contact with the electrolyte is made and then raised to develop a hanging meniscus.

It is surprising that, despite the obvious differences in the hydrodynamic boundaries imposed by the omission of the insulating shroud and the presence of a meniscus of electrolyte, the HMRD follows closely the Levich equation. Measurements for the ferro/ferricyanide redox couple on gold have shown that the hydrodynamic behaviour of the HMRD is similar to that of a conventional RDE [7, 9]. Linear plots of limiting current (i_L) against square root of rotation rate (ω) were obtained, showing the same slope as that expected for a conventional RDE and with a small negative intercept [7].

The linear variation of i_L with the square root of ω is, on the one hand, an interesting fact. On the other hand, the absence of an insulating shroud introduces

* Author to whom correspondence should be addressed.

0021-891X

potential advantages for using the HMRD configuration in systems where creating a seal at the electrode–mantle interface may be difficult and also allows application of a wide variety of treatments to the electrode surface (annealing, electropolishing etc.) before mounting. The HMRD has been used with gold [8, 10, 11] and platinum [12] single crystal electrodes, as well as in corrosion studies [13, 14], although it is only recently that its hydrodynamic behaviour has been studied experimentally in detail [9].

The absence of an insulating mantle and a meniscus of electrolyte rising above the general electrolyte level are the main features of the HMRD and it is on this basis that the hydrodynamic behaviour of this configuration was recently described [9]. The meniscus free surface imposes a clear limit to the mass transport. Once the liquid in the hydrodynamic layer reaches the disc edge, it has to change direction and flow down along the meniscus surface. This reversal of flow direction at the edge operates as a reduction of *effective radius* of the electrode for the convective diffusion current. According to Cahan [15], this perturbed layer should have a thickness similar to that of the hydrodynamic boundary layer, δ_0. Thus, the effective radius is

$$R_{\text{eff}} = R_0 - K(\nu/\omega)^{1/2} \tag{1}$$

where R_0 is the geometric radius and K is a proportionality constant [15].

We have recently studied the hydrodynamic behaviour of the HMRD by varying experimental parameters such as electrode material, electrode diameter and meniscus height [9]. A correction term was introduced into the Levich equation to account for the reduction of effective electrode radius promoted by the change in flow direction [15]. From this [9],

$$i_{\text{L (HMRD)}} = 0.620\,nFD_0^{2/3}\nu^{-1/6}C_0^*\omega^{1/2}\pi R_0^2 \times [1 - 2KR_0^{-1}(\nu/\omega)^{1/2}] \tag{2}$$

where R_0 is the geometric radius, K is a proportionality constant and all the other symbols have their usual meaning [16, 17]. The first term in Equation 2 is the standard Levich equation and the second term, which does not depend on rotation speed and accounts for the negative intercept, is given by

$$\text{Intercept} = -[0.620\,nFD_0^{2/3}\nu^{-1/6}C_0^*A] \times 2KR_0^{-1}\nu^{1/2} \tag{3}$$

where the amount indicated between brackets is the slope of the standard Levich equation.

The validity of Equation 2 has been demonstrated [9] and explains the slope value and the negative intercept. The thickness of the flow reversal region was shown to be a function of rotation speed, meniscus height and electrode radius. The value of the proportionality constant, K, depends on meniscus height (h_m) as follows:

$$K = k(h_m - h_0) \tag{4}$$

where h_0 corresponds to the value of critical meniscus height above which h_m should be set to prevent meniscus climb on the cylinder side [9] (at and below h_0 lateral wetting is expected to occur and Equation 2 is no longer valid). The values of k and h_0 were found to depend on specific properties of the electrode–meniscus interface [9].

Further evidence of the validity of Equation 2 was obtained in the application of the HMRD to the study of the kinetics of simple charge transfer reactions under mixed control [18]. It was found that employing the usual methodology to extract quantitative kinetic information for charge transfer reactions based on the method of Frumkin and Tedoradse [19] for the RDE, that is, plotting $1/i$ against $\omega^{-1/2}$ for first-order kinetics, nonlinear plots were obtained for the HMRD configuration. However, it was demonstrated [18] that the general equation for first-order kinetics,

$$\frac{1}{i} = \frac{1}{i_{\max}} + \frac{1}{i_L} \tag{5}$$

is also valid for the HMRD (the equivalent equations for reaction orders other than one also hold) [18]. The kinetic current, $i_{\max}$, obtained on the HMRD at any given potential and for any h_m set above h_0, is identical to that obtained using a conventional RDE (this also applies to the potential region close to equilibrium) [18].

In the present work, the influence of meniscus height and rotation rate on the shape of the meniscus free surface and its relation to the lateral wetting problem is studied. Experimental observations regarding meniscus instability are also made.

2. Experimental details

Experiments were carried out on Au, Pt, Cu and graphite electrodes of different sizes. They were mounted in an HMRD configuration as described elsewhere [7]. A conventional gold RDE (Pine Instruments) was used for comparison.

Electrochemical runs were carried out using the ferro/ferricyanide redox couple as test reactions (5×10^{-3} M ferro/ferricyanide in 1 M Na_2SO_4). Solutions were prepared from AR reagents and ultra pure water produced by a MilliRo-MilliQ system. A glass cell for rotating electrodes (Pine Instruments) was employed. A gold sheet separated by a glass frit served as counter electrode. All potentials were measured against a SCE.

All experiments were performed using an AFSR Pine Rotator. Runs were made at different rotation rates ranging from 400 to 10 000 r.p.m.. Meniscus height was carefully measured by using a dial gauge mounted through an adaptor to the rotor [7].

Changes in the shape of hanging meniscii of different heights and at different rotation speeds were followed photographically. Pictures were taken for meniscii established on a Petri dish, with the camera mounted on a tripod at aproximately the level of the surface and using a set of close-up lenses. Magnification of one-half was obtained [20]. Images were

scanned and computer processed to get clearer and enlarged profiles.

3. Results and discussion

3.1. *Lateral wetting and hydrodynamic behaviour*

Figure 1 shows the Levich plots for ferricyanide reduction on a 0.30 cm diameter gold electrode at different meniscus heights and the corresponding curve for the conventional gold RDE (only selected meniscus heights are shown). As can be seen, for the higher meniscii the Levich curve has the same slope, within a few percent, as that of the conventional RDE and shows a small negative intercept, in agreement with previously published data [7, 9]. The different behaviour of the smaller meniscus (0.07 cm) has been explained by using Equations 1–4 [9]. When $h_m = h_0$, the effective radius equals the geometric radius of the disc and thus Equation 2, which gives the i_L/ω dependence for the HMRD, reduces to the conventional Levich equation. For any h_m above h_0, Levich plots show a negative intercept and the slope

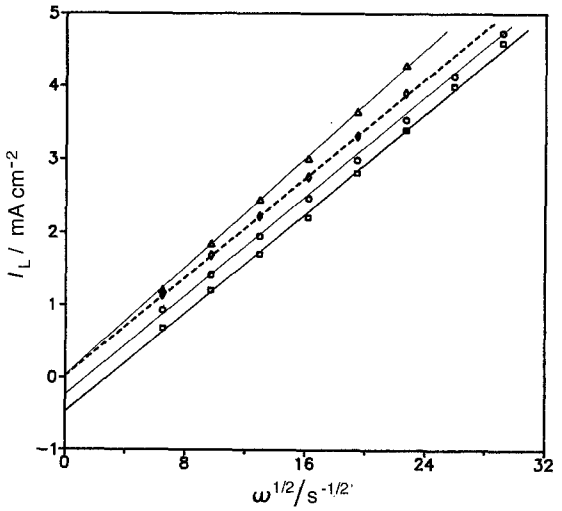

Fig. 1. Levich plots for ferricyanide reduction at a 0.30 cm diameter Au electrode at different meniscus heights: (△) 0.070, (○) 0.200 and (□) 0.237 cm. The corresponding curve for a conventional RDE is included for comparison (dashed line).

equals that expected for a conventional RDE, while for any value of meniscus height smaller than h_0, Equation 2 will no longer describe the system behaviour. Below h_0 lateral wetting occurs (the calculated value of h_0 for the 0.30 cm diameter gold electrode in this electrolyte was ≈0.14 cm) [9]. If a layer of electrolyte wets the cylinder side and remains during rotation, the situation is then equivalent to having an electrode of larger area than that of the cylinder base and it is clear that a small increase in the slope of a Levich plot should be expected.

3.2. *Shape of the meniscus free surface*

Visual inspection of the shape of the free meniscus surface shows that it changes as meniscus height is increased. In general, when a hanging meniscus of electrolyte has to be set for a given experiment, a dry electrode is lowered until contact with the electrolyte is made. At this point, the liquid wets the cylinder side in similar fashion to what is observed in Neumann's method (the Wilhelmy slide technique) for measurement of contact angles [21]. When the electrode is raised above the general level of the electrolyte to develop a hanging meniscus, a continuous change of the local contact angle, that is, the angle between the electrolyte and the cylinder side, θ_L, is observed. When the meniscus height is small, it is possible to observe that the electrolyte keeps wetting the side of the cylinder. When the electrode is raised, the liquid slides down the sides of the cylinder until only the disc surface is wet. A further increase in h_m produces a meniscus that is limited at the edge of the disc and hangs down perpendicularly to the electrode surface. Above this point, the meniscus is constrained at its centre. Hanging meniscii at different heights are shown in Fig. 2.

All photographs were scanned and processed by computer in order to obtain clearer profiles of the meniscus free surface. These enlarged profiles were put together by taking the electrode surface as reference level (for photographs taken at h_m close to or below h_0 the limit electrolyte–metal was considered as equivalent to the electrode surface, although it

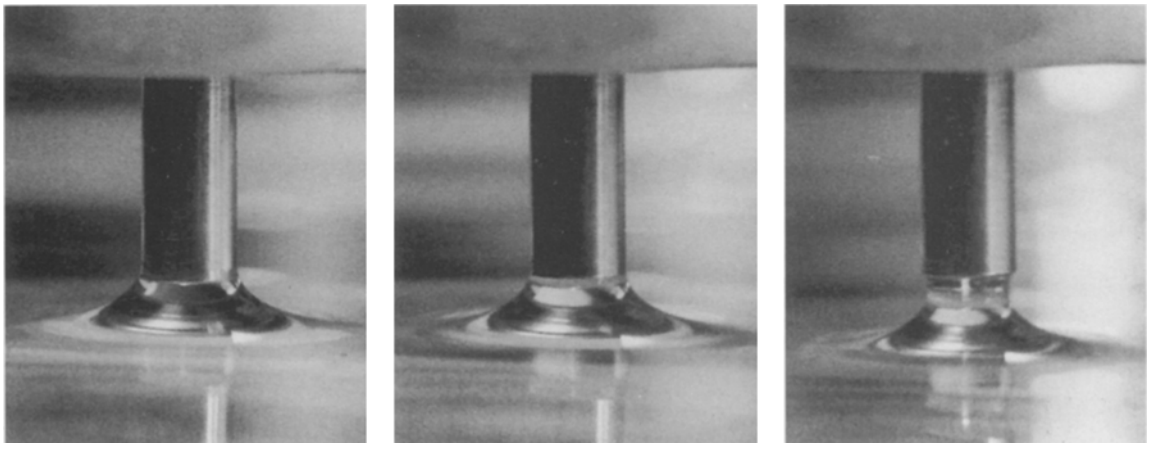

Fig. 2. Hanging meniscus at different heights on a 0.30 cm diameter Pt electrode. Meniscus heights: 0.061 (left), 0.162 (middle) and 0.226 cm (right). (Hanging meniscii appear not being axisymmetric because of light placement.)

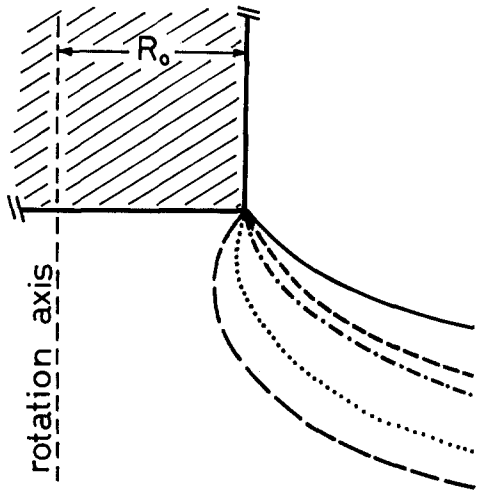

Fig. 3. Profiles of hanging meniscii of different heights, h_m, on a 0.30 cm diameter Pt electrode: (——) 0.0.61, (– – – –) 0.139, (–·–·–) 0.162, (·····) 0.209 and (— — —) 0.226 cm.

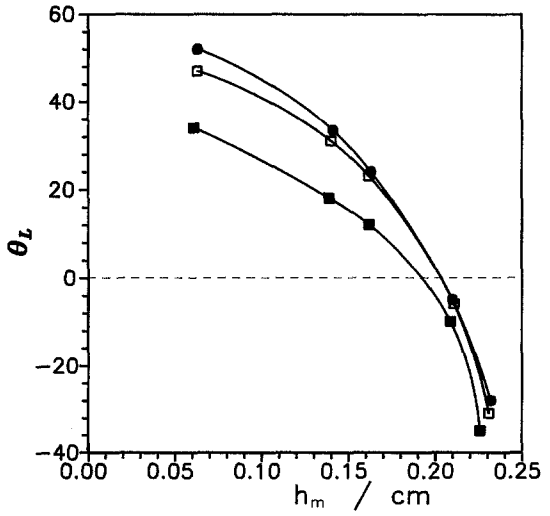

Fig. 4. Dependence of local contact angle obtained for electrodes of 0.30 cm diameter at meniscus heights h_m: (■) Pt, (●) Au, (□) graphite.

was easy to see that a small portion of the cylinder side was wet). Figure 3 shows the meniscus profiles for different heights. As can be seen, the local contact angle, θ_L, decreases for higher values of h_m. The dependence of the local contact angle on meniscus height is shown in Fig. 4 for different electrode materials of the same diameter. It is worth noting the clear shift obtained for Pt with respect to Au and graphite.

3.3. *Meniscus shape under rotation*

The shape of the hanging meniscus changes considerably under rotation. For small values of h_m the shape of the meniscus free surface is only slightly changed by rotation. However, for a meniscus that is high enough to show constriction at its centre, rotation alters the shape of the meniscus free surface in a dramatic way, particularly at high rotation speeds, as shown in Fig. 5. Enlarged profiles obtained at several rotation rates for a hanging meniscus set at $h_m = 0.23$ cm on a platinum cylinder are shown in Fig. 6.

It is obvious that the amount of liquid that can be sustained above the general level is increased by rotation. The centrifugal force exerts a pressure that pushes the liquid free surface outward, producing a considerable change in the shape of the meniscus. Rotation also affects θ_L which varies linearly with $\omega^{1/2}$ as shown in Fig. 7 for three different electrode materials of identical diameter.

3.4. *Meniscus climb on the cylinder side*

3.4.1. Volume of liquid above the general level. Meniscii at a free liquid surface have also been widely used in several methods employed in the measurement of surface tension of liquids [21–23]. One method consisted in the determination of the maximum pull on a rod [22]. From simple physical laws, Padday *et al.* [22] proposed that the force in excess of the weight of the rod is exactly equal to the weight of liquid raised above the general level according to

$$f = \pi R_0^2 h_m \rho g + 2\pi R_0 h_m \gamma \sin\phi \qquad (6)$$

where ρ is the density difference between the liquid and its surrounding fluid, g is the gravitational acceleration, γ is the surface tension of the liquid and ϕ is the angle of the meniscus with the horizontal, as

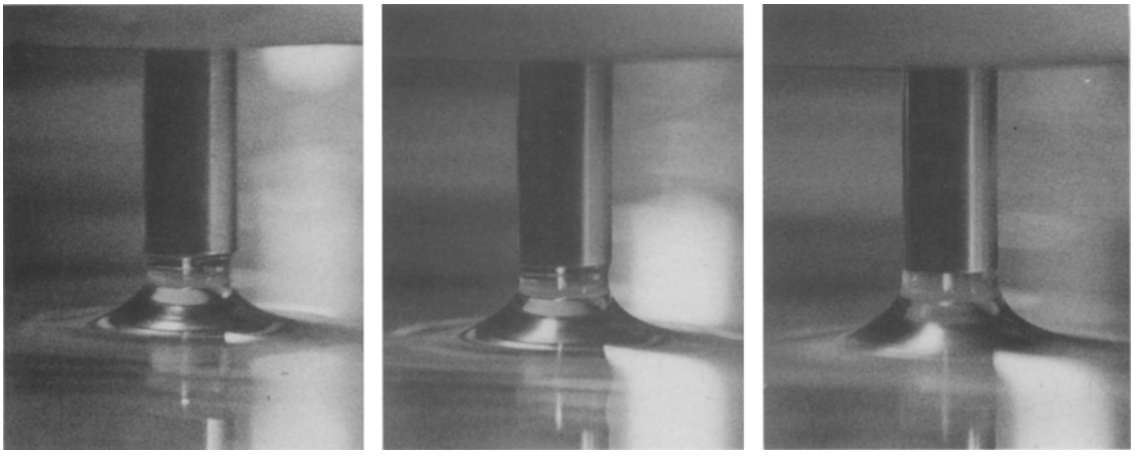

Fig. 5. Hanging meniscus on a 0.30 cm Pt electrode at different rotation rates (r.p.m.): 0 (left), 4000 (middle) and 10 000 (right). $h_m = 0.226$ cm.

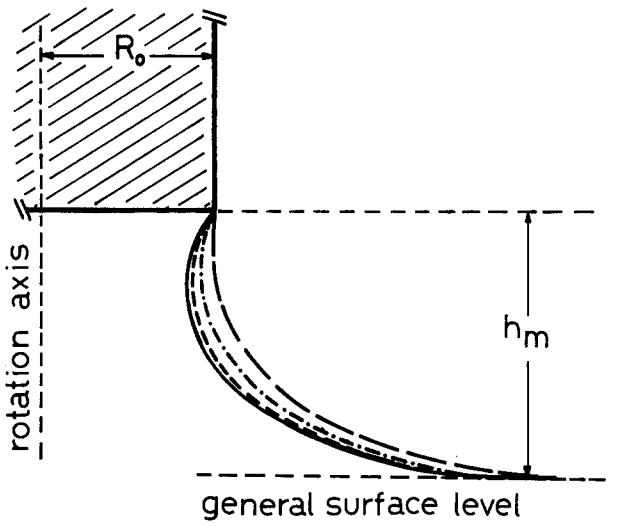

Fig. 6. Profiles of hanging meniscii on a 0.30 cm diameter Pt electrode at different rotation rates (r.p.m.): (——) 0; (– – – –) 2000; (– · – · –) 4000; (— —) 8000. $h_m = 0.226$ cm.

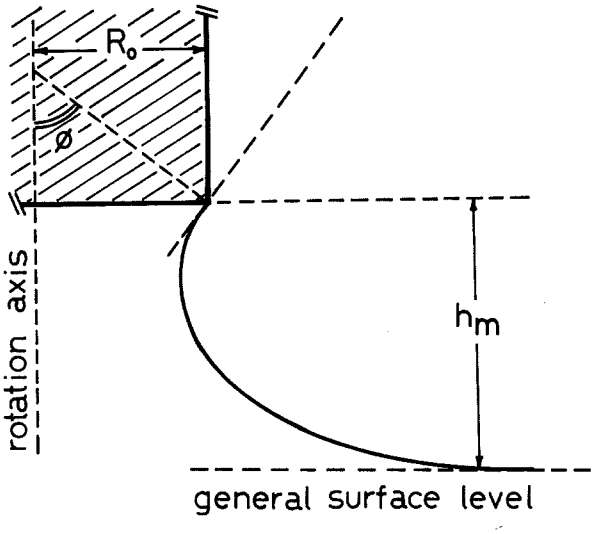

Fig. 8. Schematic diagram showing the angle ϕ.

defined in Fig. 8. The first term represents the hydrostatic pressure of the liquid and the second term the force arising from the surface tension pull around the edge. The volume of liquid above the general surface ($F/\rho g$) [22] can be then calculated from

$$V = \pi R_0^2 h_m + \frac{2\pi R_0 h_m \gamma \sin\phi}{\rho g} \qquad (7)$$

By using the local contact angles measured from the photographs, the volume of liquid above the general surface can be calculated from Equation 7 (note that $\phi = \theta_L + 90°$). This volume is plotted against meniscus height for different electrode materials in Fig. 9. It can be seen that the volume of liquid above the general level increases with meniscus height, reaches a maximum, and then decreases (meniscus constriction). It is also clear from the figure that at any h_m below the value that corresponds to the maximum volume, the volume of liquid that can be sustained is higher for platinum than for gold and graphite, due to its more 'hydrophilic' nature. For higher meniscii, the opposite effect is observed, Pt being the material that shows the smaller values of volume in this region. This is not surprising since when the meniscus begins to show constriction, the interaction between the electrolyte and the metal is limited to the base of the cylinder. Consequently, meniscus constriction should be more pronounced if the liquid tends to spread over ('wet') the surface. Maximum volume is almost independent of electrode material in agreement with Padday's results [22].

3.4.2. Lateral wetting for static meniscus. While running the experiments, it was observed that the range of meniscus heights that could be set for platinum was narrower than that for gold. This difference is clearly associated with the more 'hydrophilic' nature of platinum as compared with gold or graphite. In the region of low values of h_m, the limit is set by the value of h_0 and it has been found that h_0 for Pt (~0.16 cm) is higher than for Au (~0.14 cm) [9]. On the other hand, Figs 4 and 9 indicate that after the

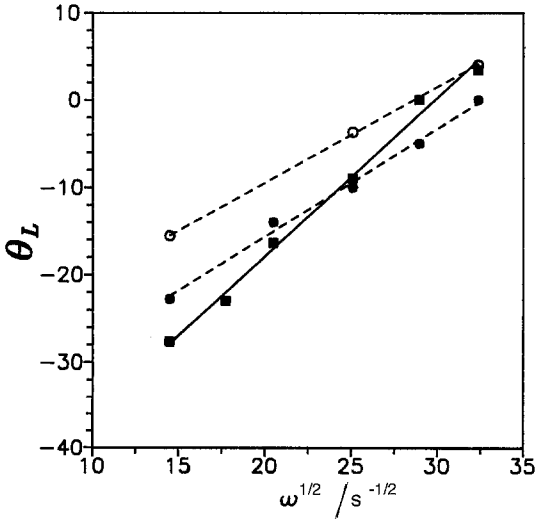

Fig. 7. Local contact angle against $\omega^{1/2}$ for 0.30 cm diameter electrodes: (■) Pt ($h_m = 0.226$ cm), (●) Au ($h_m = 0.228$ cm) and (○) graphite ($h_m = 0.231$ cm).

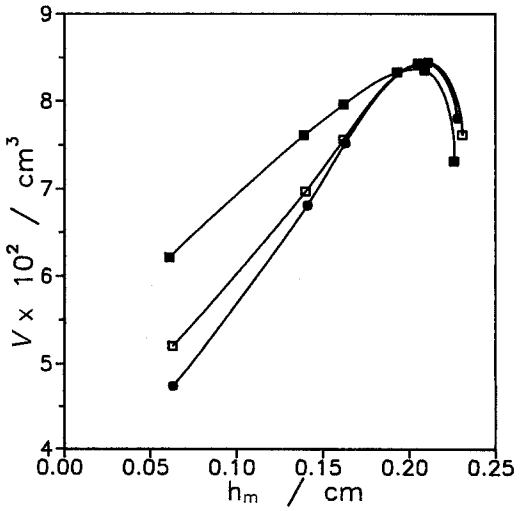

Fig. 9. Volume above the general surface level calculated from Equation 7 against h_m for 0.30 cm diameter electrodes: (■) Pt; (●) Au; (□) graphite.

maximum volume is reached, the hanging meniscus on platinum will show a more pronounced constriction at its centre. Consequently, less stability should be expected since these meniscii tend more rapidly towards the point of rupture.

It is also evident from Fig. 9 that the volume above the general level does not fall to zero for $h_m = 0$. In fact, this should be expected because when a dry electrode is brought into contact with the electrolyte, the liquid 'jumps' to wet the side. Values of the volume above the general surface obtained by extrapolation to $h_m = 0$ are almost identical to those calculated assuming that the situation at $h_m = 0$ is similar to having the rod immersed in the electrolyte as in the Wilhelmy slide technique [21], i.e. taking $\phi = \theta_C + 90°$ (where θ_C is the 'normal' contact angle corresponding to the electrode material in the electrolyte [18]). This agreement can be taken as a crude indication that setting $h_m = 0$ is, in fact, equivalent to having the electrode immersed (i.e. $\theta_L = \theta_C$). Thus, for $h_m = 0$ the height of the wetted portion on the electrode side can be estimated from the same equation used for a partially immersed plate on which the meniscus rises to a definite height, h, according to [21]

$$\sin\theta_C = 1 - \frac{\rho g h^2}{2\gamma} \tag{8}$$

The values obtained from Equation 8 using θ_C values taken from the literature [21] are 0.113 cm for gold and 0.230 cm for platinum. It is evident that, for any h_m in the region $0 < h_m < h_0$, lateral wetting occurs and its extent depends on the particular properties of the metal.

On the other hand, and since the slope of a Levich plot is proportional to the electrode area, lateral wetting will produce slope values higher than those expected for the area of the cylinder base. Thus, different values of slope should be observed in the region $h_m < h_0$ due to the variation of the wetted area on the side [9]. In a recent paper [24], Levich plots showing zero intercepts and considerable variation in slope have been reported. The analysis of those data clearly indicates that they were taken at meniscus heights well below the point where extensive lateral wetting occurs. Consequently, the suggestions made by these authors [24] about the 'proper experimental conditions' for using the HMRD configuration are incorrect.

3.4.3. Rotation induced lateral wetting. Although changes in the shape of the meniscus free surface are less pronounced for small meniscii, the excess pressure exerted by the centrifugal force on the liquid interface should have similar consequences at any meniscus height. In other words, an increase in the local contact angle caused by rotation should always be expected. This means that, even if no lateral wetting is apparent for a given value of h_m for a static meniscus, a certain value of rotation speed may produce a local contact angle that approaches θ_C of the electrode material allowing the liquid to creep up the vertical wall. This type of rotation induced lateral wetting was actually observed and caused, in general, meniscus instability, particularly on platinum. In some cases, this liquid on the cylinder wall could not be sustained during rotation and was thrown outward, producing immediate rupture of the hanging meniscus. Attention should be paid to the fact that the local contact angle changes with rotation more rapidly for platinum than for materials that are less hydrophilic (gold and graphite) as is shown in Fig. 7. Lateral wetting induced by rotation should be expected to occur more easily (at lower rotation speeds) on hydrophilic materials.

3.5. *Conditions for proper use of the HMRD*

It is clear that the HMRD will be properly used only when the meniscus does not wet the cylinder side. When this condition is fulfilled the behaviour of the HMRD is described by Equation 2; a negative intercept should be observed in Levich plots, while the slope should be the same as that of a conventional RDE [9]. Changes in slope are indicative of lateral wetting whose extent varies with meniscus height for all values of h_m below h_0. All measurements should be carried out at meniscus heights that are above the critical height h_0. If h_0 for the system under study is unknown, the presence of a negative intercept on Levich plots may be taken as a crude indication of an adequate meniscus height [9].

If mass transport is being studied, measurements should be taken at a constant value of h_m. Measurement of h_m can be done in a very simple way [7]. However, for other types of experiments, measurement of meniscus height is not always required. For instance, in studies of the kinetics of simple charge transfer reactions, results were independent of meniscus height as long as the liquid did not creep up the electrode side [18]. If the electrode is raised to establish a meniscus that shows constriction, lateral wetting should not occur even at high rotation speeds. Therefore, visual inspection might be sufficient. Special attention should be paid to the lateral wetting problem in the case of single crystal electrodes where meniscus climb introduces spurious contributions from other crystal faces.

4. Conclusions

The shape of the meniscus free surface changes considerably with meniscus height and consequently, the local contact angle (θ_L) also depends on h_m . For meniscii set at h_m ranging from 0 to h_0, the liquid wets the electrode side despite the decrease observed for the local contact angle. The extent to which wetting occurs at any given value of h_m within this range depends on the nature of the electrode material. Above h_0 no lateral wetting is expected for a static meniscus.

Electrode rotation produces a strong variation on the shape of the meniscus free surface and an increase in the local contact angle that may produce meniscus climb. This rotation induced lateral wetting should, in

principle, be expected to occur on 'hydrophilic' materials such as platinum and for meniscus heights close to h_0. The amount of liquid sustained by the electrode above the general surface increases with rotation rate, and may cause a drop in the local level of the electrolyte producing meniscus instability and/or rupture.

Electrochemical measurements should always be carried out at meniscus heights that are above the critical height h_0. However, careful measurement of h_m might not always be necessary and could be replaced by visual inspection. A hanging meniscus that shows constriction at its centre ensures that lateral wetting will not occur, even at high rotation speeds.

Acknowledgements

This research was supported by CONICET, CONICOR and SECYT(UNC).

References

[1] V. G. Levich, 'Physicochemical Hydrodynamics', Prentice Hall, Englewood Cliffs, NJ (1962).
[2] A. C. Riddiford, *in* 'Advances in Electrochemistry and Electrochemical Engineering', Vol. 4, Interscience, New York (1966).
[3] R. N. Adams, 'Electrochemistry at Solid Electrodes', Marcel Dekker, New York (1969).
[4] F. Opekar and P. Beran, *J. Electroanal. Chem.* **69** (1976) 1.
[5] D. Dickertmann, F. D. Koppitz and J. W. Schultze, *Electrochim. Acta* **21** (1976) 967.
[6] A. Hamelin, *in* 'Modern Aspects of Electrochemistry', Vol. 16, (edited by B. E. Conway and J. O'M. Bockris), Plenum Press, New York, (1986).
[7] B. D. Cahan and H. M. Villullas, ECS Meeting, Chicago (1988), Abstract 707; B. D. Cahan and H. M. Villullas, *J. Electroanal. Chem.* **307** (1991) 263.
[8] B. D. Cahan, H. M. Villullas and E. B. Yeager, ECS Meeting, Atlanta (1988), Abstract 532; B. D. Cahan, H. M. Villullas and E. B. Yeager, *J. Electroanal. Chem.* **306** (1991) 213.
[9] H. M. Villullas and M. López Teijelo, 43rd ISE Meeting, Córdoba, Argentina, 1992, Abstract 6–014; H. M. Villullas and M. López Teijelo, *J. Electroanal. Chem.* **384** (1995) 25.
[10] B. D. Cahan, H. M. Villullas and E. B. Yeager, unpublished results.
[11] R. R. Adzic, J. Wang and B. M. Ocko, *Electrochim. Acta* **40** (1995) 83.
[12] F. H. Feddrix, E. B. Yeager and B. D. Cahan, *J. Electroanal. Chem.* **330** *(1992) 419.*
[13] M. M. Laz, R. M. Souto, S. González, R. C. Salvarezza and A. J. Arvia, *Electrochim. Acta* **37** (1992) 655.
[14] R. M. Souto, M. Pérez Sánchez, M. Barrera, S. González, R. C. Salvarezza and A. J. Arvia, *ibid.* **37** (1992) 1437.
[15] B. D. Cahan, Proceedings of the Symposium on Modelling of Batteries and Fuel Cells, ECS Meeting, Phoenix (1991).
[16] A. J. Bard and L. R. Faulkner, 'Electrochemical Methods', J. Wiley & Sons, New York (1980).
[17] E. Gileadi, 'Electrode Kinetics', VCH, Weinheim/New York (1993).
[18] H. M. Villullas and M. López Teijelo, *J. Electroanal. Chem.* **385** (1995) 39.
[19] A. Frumkin and G. Tedoradse, *Z. Elektrochem.* **62** (1958) 251.
[20] W. White, Jr., 'Close-up photography', the Kodak Workshop Series, Eastman Kodak Company, New York (1984).
[21] A. W. Adamson, 'Physical Chemistry of Surfaces', 4th edn, Wiley Interscience, New York (1982).
[22] J. F. Padday, A. R. Pitt and R. M. Pashley, *J. Chem. Soc. Faraday Trans. I* **71** (1975) 1919.
[23] D. J. Shaw, 'Introduction to Colloid and Surface Chemistry', Butterworth-Heinemann, Oxford (1992).
[24] C. I. Elsner, P. L. Schilardi and S. L. Marchiano, *J. Appl. Electrochem.* **23** (1993) 1181.